ISSN:3007-9640 DOI: https://doi.org/10.70114/acmsr.2025.3.1.P258

Design and Simulation Analysis of Civil Aircraft Cockpit Door Test Bench

Jie Ren [1, 2], Xiaohu Zeng[1,2], Yang Wu [1, 2, a], and Chunyu Bai [3]

[1] State Key Laboratory of Airliner Integration Technology and Flight Simulation, Shanghai, 201210, China;

[2] COMAC Shanghai Aircraft Design & Research Institute, Shanghai, 201210, China;

[3] National Key Laboratory of Strength and Structural Integrity, Xi’an, 710065, China.

[a] wuyang_0304@126.com

Abstract. Aircraft cockpit doors may experience electric strike disengagement difficulties due to fuselage pressurization-induced deformation, potentially leading to door operation failures in critical scenarios. To address this issue, this paper develops a test bench capable of simulating deformation patterns. Through computational analysis, a test bench structure that meets the functional requirements was obtained, providing a reference for similar designs while offering practical support for utilization in testing under deformation conditions.

Keywords: Cockpit Door; Test Bench Design; Load Analysis.

1. Introduction

The cockpit door in aircraft is located between the cabin and the cockpit, serving to isolate these two areas. In addition to allowing normal crew access, it incorporates bulletproof and intrusion-resistant features to prevent unauthorized personnel from forcibly entering the cockpit. The door also automatically activates its pressure relief panel during cabin depressurization to balance pressure differentials between the cockpit and cabin[1]. Furthermore, it provides lock/unlock control and a status display for door opening/closing.

The cockpit door typically consists of door structural components, door locks and control system, in which door structural components include door plate, pressure relief plate, hinges and door frame, etc. Door locks include door solenoid locks and pressure relief induction locks, and the control system includes control panel, electrical control box, password board, indicator light and loudspeaker[2].The structure of the cockpit door is shown in Fig. 1, and the control system architecture is depicted in Fig. 2.

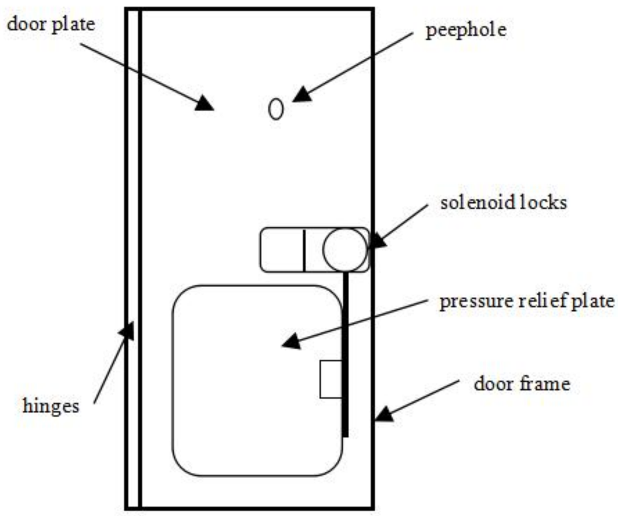

Fig. 1 Schematic diagram of cockpit door structural components

ISSN:3007-9640 DOI: https://doi.org/10.70114/acmsr.2025.3.1.P258

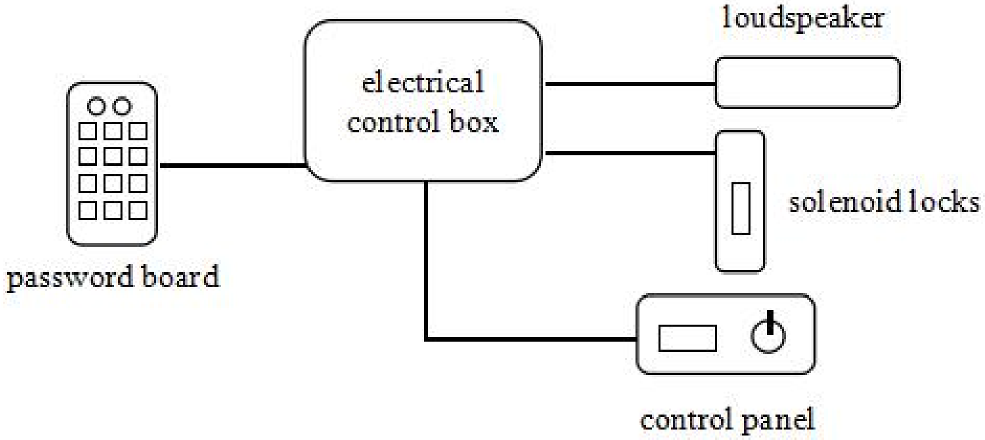

Fig. 2 Control system architecture

The password board is installed on the cockpit door near the passenger cabin side. Cabin crew members can input the password to send an entry request, and at the same time, there is also an indicator light on the password board, which is used to prompt the current status of the cockpit door. The door controller outputs warnings and status information through visual indicators and audible alarms, alerting crew members to entry requests or system abnormalities. The control panel is mounting plated on the center console in the cockpit, and both pilots can manipulate the cockpit door to lock or unlock [3]. Electric strike is the locking mechanism of the door, when it is in the locked state, the cockpit door will not be able to open, when the electric strike is in the unlocked state, personnel outside the cockpit can open the cockpit door. When the cabin crew finds that there is an accident in the cockpit and needs to enter the cockpit, they can use the emergency entry program, and the cabin side crew can unlock the electric strike by entering the emergency code.

When the aircraft is in the air, the fuselage deforms under the action of pressurized load, which causes a significant increase in the contact force between the cockpit door latch and the column stopper, resulting in the electric strike being unable to overcome the friction and unlocking the lock, which can lead to an extremely serious safety accident if the cockpit crew is disabled at this time. The best way to solve this problem is to carry out the relevant test verification for the cockpit door electric strike, in the case of cockpit door deformation under pressure, carry out the electric strike unlocking operation, to see whether it fails.

At present, the conventional practice relies on flight testing or computational simulation. While flight test provides the most authentic operational data, it remains time-consuming, labor-intensive, and cost-prohibitive. Simulation analysis, though theoretically useful, cannot fully replace physical testing due to its inherent limitations in modeling the dynamic electric strike disengagement process, which significantly increases implementation complexity. To address these challenges, this study develops a cockpit door test bench. After acquiring door deformation data through flight tests or simulations, the apparatus enables precise replication of in-flight deformation states on test bench, thereby establishing controlled experimental conditions for electric strike performance.

2. Test Bench Overview

The test bench consists of a main frame, a loaded deformation module, a spindle and connectors, as shown in the figure below. The column side and hinge side of the cockpit door are connected to the simulated mounting plate, and the fastener opening and size on the mounting plate should be consistent with the real aircraft to ensure the effect when simulating deformation.

ISSN:3007-9640 DOI: https://doi.org/10.70114/acmsr.2025.3.1.P258

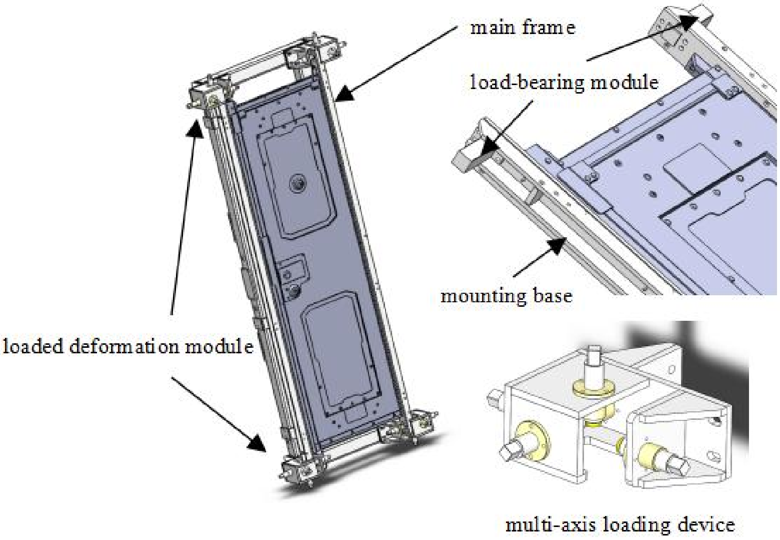

Fig. 3 Schematic diagram of the test bench

Among them, the loading deformation module consists of a multi-axis loading device and a load-bearing module, in which the multi-axis loading device is not directly loaded on the mounting plate, but is loaded on the load-bearing module, which is connected to the mounting plate, and the load-bearing module is subjected to displacement by the loading force, which leads to a change in the mounting plate and the cockpit door, which maximally reduces the deformation of the on-board pressurized load deformation resulting in the deformation of the cockpit door body around the process. The loading and deformation module is also connected with the main frame through fasteners, in addition to loading and deformation, the module also plays the role of supporting the cockpit door. In order to change the angle of the cockpit door, there is a pivot shaft on the back of the main frame, which can be used with an external power source to rotate the main frame and the cockpit door.

The main frame, rotating shaft and loading device of the loading deformation module are made of 45# steel, which has excellent tensile and yield strength, good plasticity and weldability, wear resistance, high reliability and easy cutting.

The adjusting blocks of the control jigs are made of 40Cr. The material shows good overall mechanical properties after quality treatment, including high tensile and flexural strength. At the same time, it also has excellent low-temperature impact toughness and low notch sensitivity, which makes it under heavy load or complex stress environment can still maintain stable performance.

The column mounting plates and hinge mounting plates are machined from aluminium alloy 7075-T3511. 7075-T7351 is a high strength aluminium alloy with excellent mechanical properties and corrosion resistance. The alloy belongs to the Al-Zn-Mg-Cu system and the main elements include aluminium, zinc, magnesium and copper. During the manufacturing process, 7075-T7351 aluminium alloy undergoes a special heat treatment to give it high strength and hardness. This material is widely used in aviation, aerospace, automotive, machinery, electronics and other fields, especially where large loads and complex environments are required. In addition, 7075-T7351 has good resistance to spalling corrosion and stress-corrosion fracture.

In practical application, first according to the cockpit door finite element analysis and on-board measurement results, to obtain the cockpit door deformation and angle data, and then in the frame through the loading device and the rotary axis, so that the cockpit door to obtain the corresponding deformation and angular change effect, in order to be more convenient to carry out the operation, through the main frame in the installation of distance sensors and angular sensors, to obtain the accurate deformation data and angular change data. For more convenient operation, accurate deformation data and angle change data can be obtained by installing range sensor and angle sensor in the main frame.

ISSN:3007-9640 DOI: https://doi.org/10.70114/acmsr.2025.3.1.P258

3. Simulation

To verify the reliability of the test bench loading method and ensure that neither the test bench nor the cockpit door undergoes plastic deformation, this study conducted simulation analysis using ABAQUS. The simulations modeled the loaded state of the cockpit door induced by the test bench, obtaining deformation and stress distribution data for both components after loading completion. This dual-purpose analysis confirmed the structural integrity of the bench design while validating the safety of the test specimen, laying a foundation for subsequent experimental operations.

Simulation Object

The simulation objects are the test bench and cockpit door, and the eight-node hexahedral cell is used for the main frame, mounting plate and loading module of the test bench. The eight-node hexahedral cell is able to accurately capture the complex stress gradient in the three-dimensional solid structure, and its interpolation function can more accurately simulate the nonlinear strain distribution in the area of bending, contact or local stress concentration (such as rounded corners and crack tips).Its interpolation function can more accurately simulate the nonlinear strain distribution, and its integral point distribution can accurately transfer the contact pressure, avoiding the contact force error caused by neglecting the thickness direction stress in the shell unit.

The cockpit door adopts a four-node shell cell, which is an effective mesh type for both thin-shell (thickness-to-span ratio ≤1/15) and thick-shell (thickness-to-span ratio >1/15) problems, and is simple to divide, only need to define the shell surface geometry without considering the thickness direction discretization, and supports the hierarchical definition of the material properties, which is suitable for composite material objects such as the cockpit door. The mesh division is shown in Fig. 4.

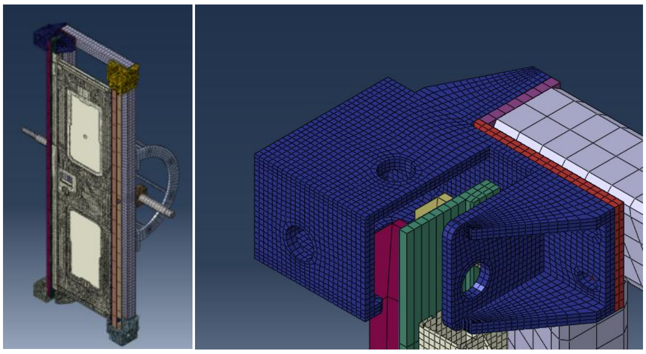

Fig. 4 Schematic diagram of grid division

The material parameters used in modelling are shown in Table 1 below.

Table 1 Material Parameters

Component	Material	Modulus of Elasticity（GPa）	Poisson's Ratio	Yield Stress（MPa）
main frame	Steel 45#	206	0.3	355
loading deformation module	Steel 45#	206	0.3	355
mounting plate	aluminium alloy 7075	72	0.33	470

Boundary Conditions

The effective means of dealing with finite element models containing contact relations in structural statics analysis lies in the correct setting of contact relations and definition of boundary conditions [4]. Most of the non-convergence problems in contact analysis are caused by the wrong setting of contact relations and unreasonable constraints on degrees of freedom. Reasonable contact relationship setting mainly includes correctly defining contact surfaces, contact properties and contact parameters, etc., while reasonable boundary conditions can ensure that the model will not produce over-constraints and under-constraints, so as to ensure that the model will not produce large rigid body displacements [5].In addition, when dealing with the model, we often encounter the problem of complex contact relationship, complex contact relationship usually leads to the simulation results of non-convergence [6], if the assembly relationship has no effect on the

ISSN:3007-9640 DOI: https://doi.org/10.70114/acmsr.2025.3.1.P258

simulation target, the reasonable use of coupling constraints instead of complex contact relationship can effectively solve the problem of non-convergence of the model, and can ensure the reliability of the simulation results. For the test stand and cockpit door connection bolt position, simulation through the ABAQUS MPC Tie instead, as shown in Figure 5 below, this treatment makes the connection of the two in the analysis of the relative displacement or rotation does not occur, equivalent to "welding" or "rigid connection". At the same time, it allows the master-slave mesh to be inconsistent, which is suitable for the mesh model in this paper.

Simulation Cases

Two critical loading scenarios were selected for finite element analysis:

1) Upper bilateral tensile loading with fixed lower constraints

2) Lower bilateral compressive loading with fixed upper constraints

These configurations represent extreme deformation patterns affecting the structural framework. This investigation acquired peak deformation values and stress distribution patterns to verify elastic deformation limits in both the main frame and mounting plate, thereby preventing plastic deformation. At the same time, discrepancies in main frame and mounting plate deformation compatibility were quantified. When deformation differentials fell within 5% tolerance thresholds, this indicated insufficient measurement resolution at primary frame locations, necessitating redesigned displacement transducer placement for effective deformation monitoring.

4. Results and discussion

Upper bilateral tensile loading with fixed lower constraints

Utilizing the Connector Displacement function within the software interface, the inter-component distance between column-side and hinge-side mounting plate was precisely increased by 3 mm, with the resultant stress distribution patterns across these components and the primary structural framework subsequent to dimensional adjustment being comprehensively documented in Figures 6-8.

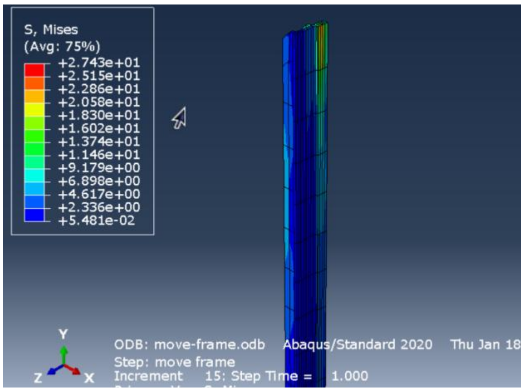

Fig. 6 Stress distribution of column-side mounting plates Fig. 7 Stress distribution of Hinge-side mounting plates

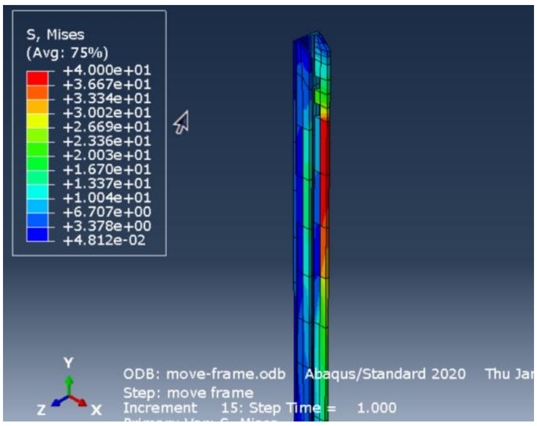

Fig. 8 Stress distribution of main frame

ISSN:3007-9640 DOI: https://doi.org/10.70114/acmsr.2025.3.1.P258

Maximum stress concentrations were identified at the mid-upper region of the primary structural framework (20.7 MPa) and the upper sections of both hinge-side (40.0 MPa) and column-side (27.3 MPa) mounting plates. All recorded stress values demonstrated significant safety margins, measuring <6% of the material yield strengths (355 MPa for the framework, 455 MPa for the mounting plates). This elastic deformation regime was conclusively verified through comparative analysis, with no plastic deformation observed across any structural components, confirming load-bearing integrity under operational conditions.

Full displacement characteristics of the primary framework are quantitatively detailed in Figures 9-11.

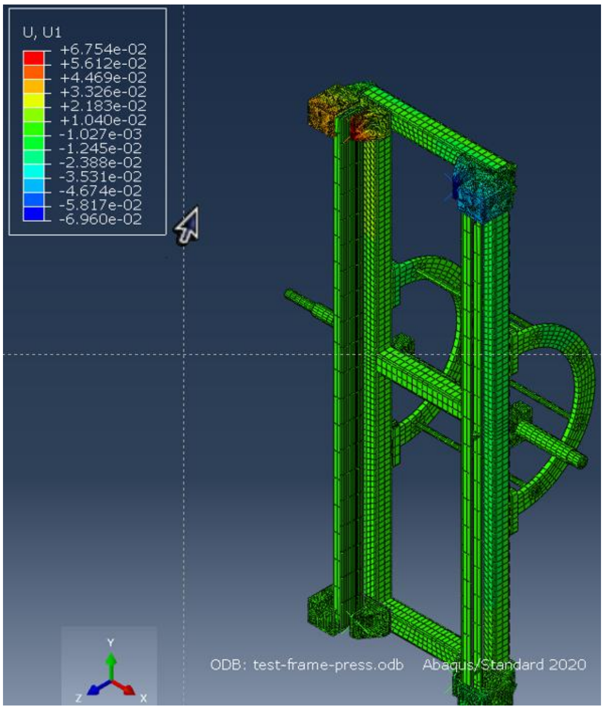

Fig. 9 X-direction displacement of main frame

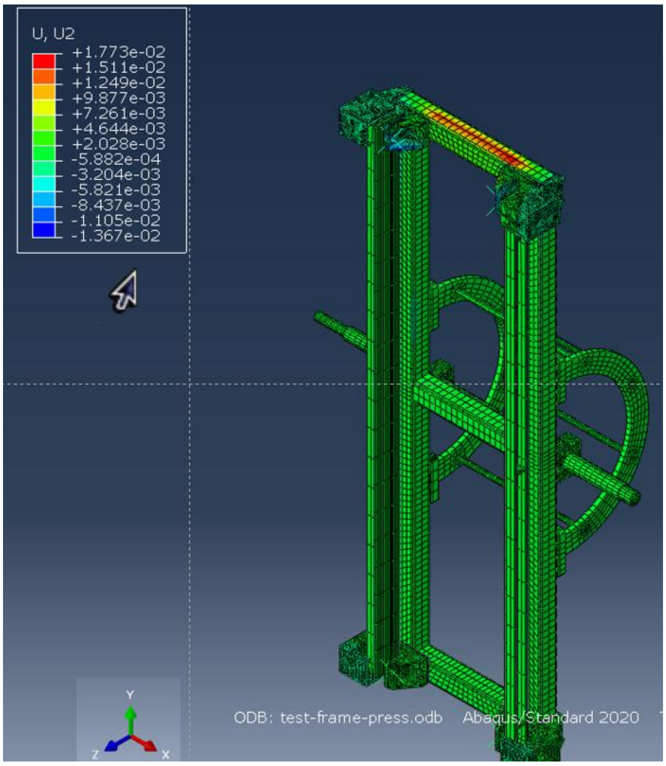

Fig. 10 Y-direction displacement of main frame

ISSN:3007-9640 DOI: https://doi.org/10.70114/acmsr.2025.3.1.P258

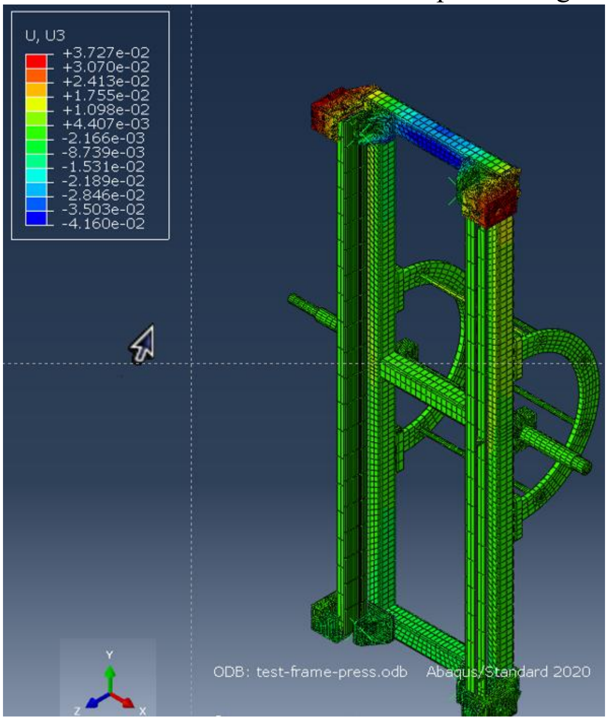

Fig. 11 Z-direction displacement of main frame

Deformation analysis revealed maximum displacements of 0.067 mm (X-direction at loading module), 0.017 mm (Y-direction at mid-upper frame), and 0.042 mm (Z-direction at mid-upper frame), with supplementary deformations ≤0.015 mm observed at bilateral upper loading module regions. All measured displacements demonstrated three-order-of-magnitude reductions compared to the 3 mm structural deformation thresholds of both the main frame and cockpit door, confirming the test bench's superior stiffness characteristics. This displacement differential validation ensures measurement system compatibility while maintaining structural integrity under operational loading conditions.

Lower bilateral compressive loading with fixed upper constraints

Utilizing the Connector Displacement function within the software interface, a controlled 3 mm compressive adjustment was applied between the column-side and hinge-side mounting plates. Post-compression stress distribution characteristics across these components and the primary structural framework are systematically illustrated in Figures 12-14.

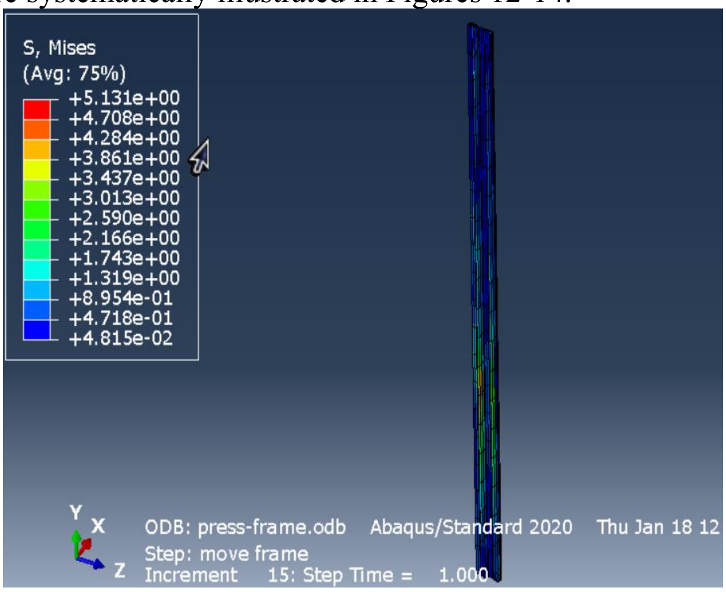

Fig. 12 Stress distribution of column side mounting plate

ISSN:3007-9640 DOI: https://doi.org/10.70114/acmsr.2025.3.1.P258

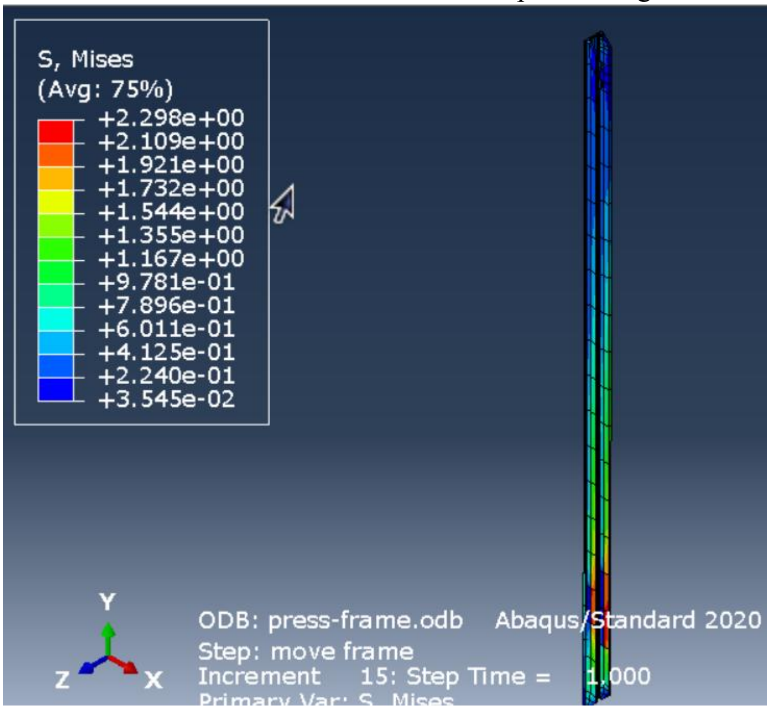

Fig. 13 Stress distribution of hinge-side mounting plate

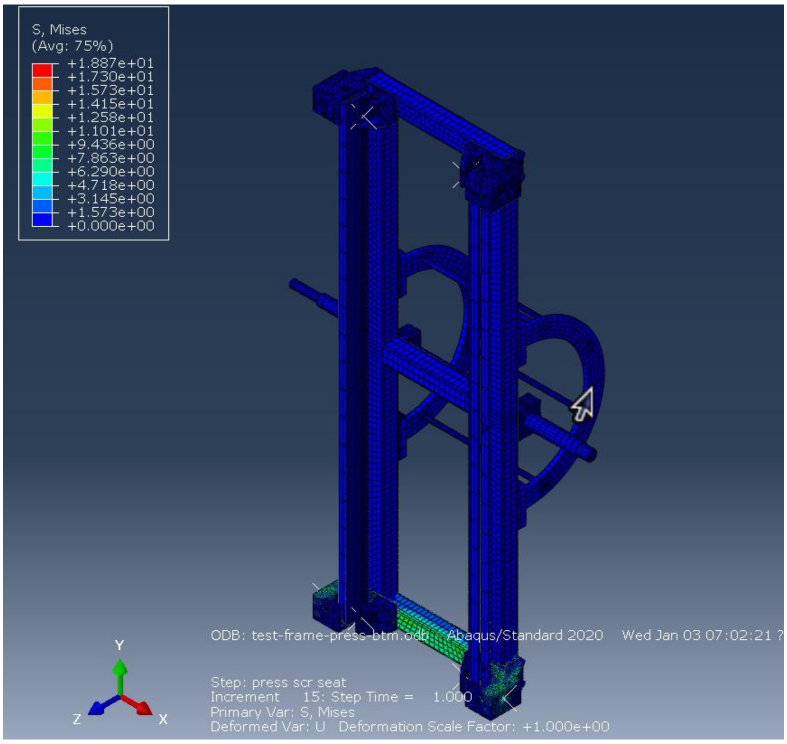

Fig. 14 Stress distribution of main frame

Stress analysis identified peak values of 18.9 MPa (mid-lower framework region), 2.30 MPa (lower hinge-side plate), and 5.13 MPa (lower column-side plate), all measuring <5.3% of respective material yield strengths (355 MPa framework / 455 MPa mounting plates). Elastic deformation dominance was conclusively verified through comparative strain evaluation, with no plastic deformation detected across any structural elements, confirming structural stability under operational loads.

The displacement of the main frame is shown in Figures 15 to 17 below.

ISSN:3007-9640 DOI: https://doi.org/10.70114/acmsr.2025.3.1.P258

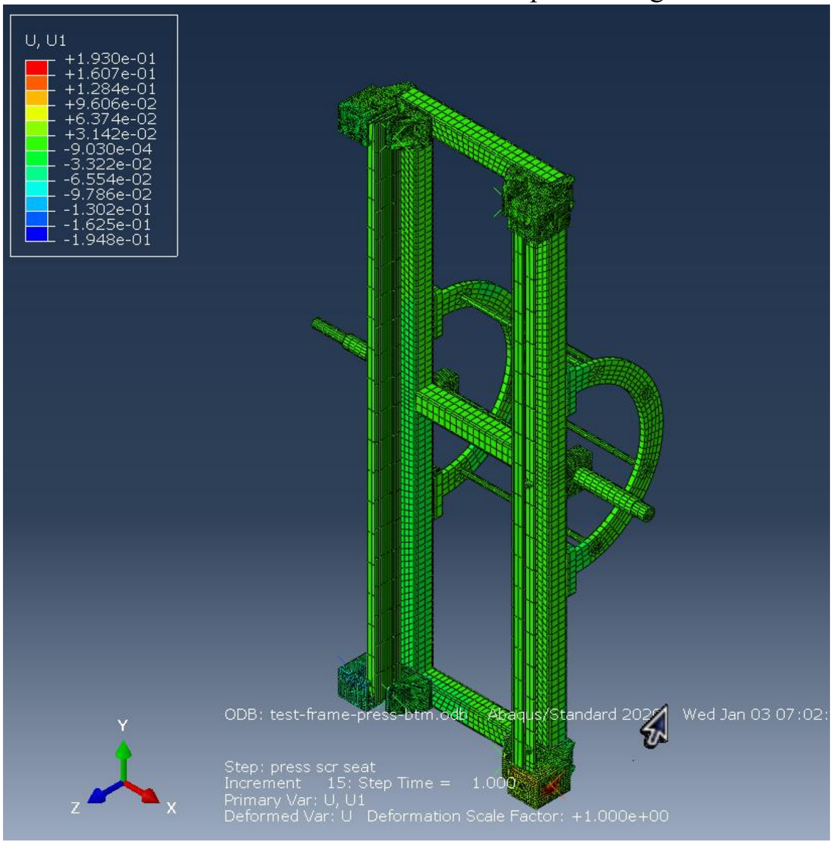

Fig. 15 X-direction displacement of main frame

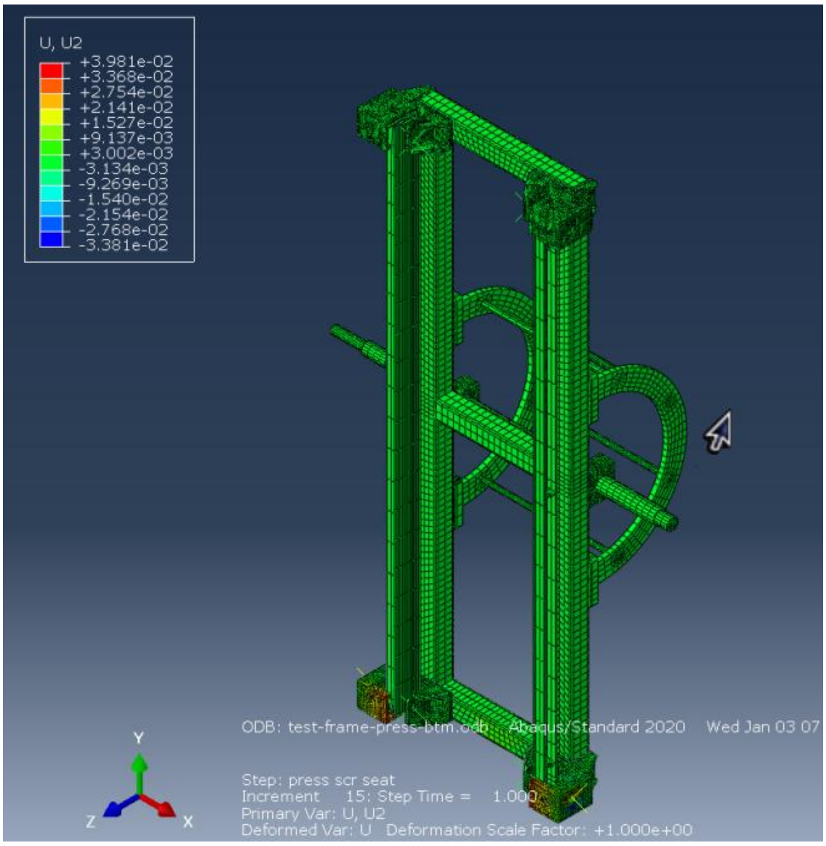

Fig. 16 Y-direction displacement of main frame

ISSN:3007-9640 DOI: https://doi.org/10.70114/acmsr.2025.3.1.P258

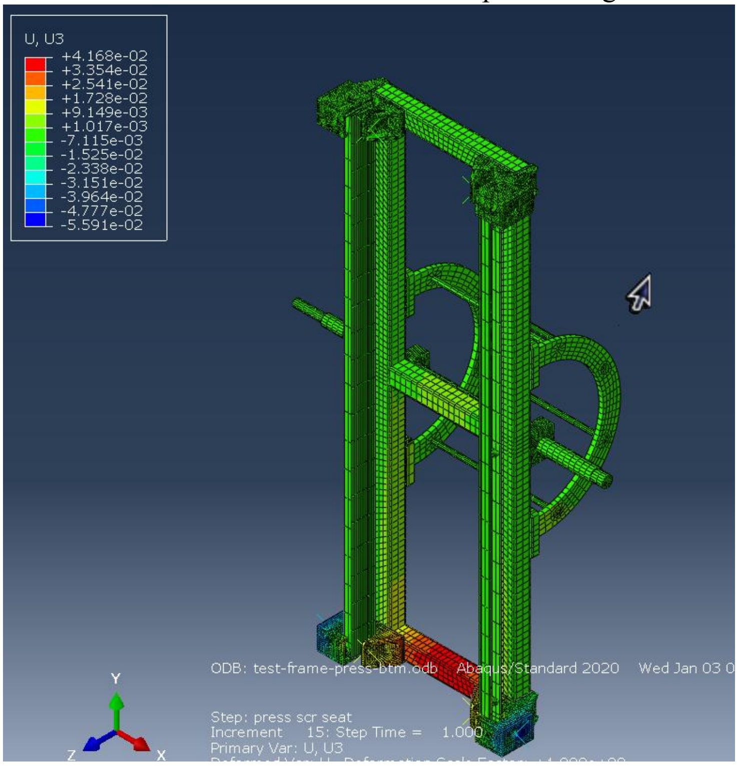

Fig. 17 Z-direction displacement of main frame

Deformation analysis revealed multidirectional displacement characteristics with maximum magnitudes of 0.19 mm (X-axis, bilateral lower loading module), 0.04 mm (Y-axis, bilateral lower loading module), and 0.04 mm (Z-axis, mid-lower framework region). Notably, opposing deformation vectors were observed between the upper loading module sectors (⩽0.015 mm) and the mid-lower framework zone, demonstrating counteractive displacement patterns. All measured deformations exhibited three-order-of-magnitude reductions relative to the 3 mm structural compliance thresholds of both the airframe framework and cockpit door assembly. Comparative stiffness evaluation confirmed enhanced mechanical performance across principal axes, with elastic deformation dominance (stress-strain ratios <5% of material yield limits) validating structural integrity under operational loading conditions.

5. Summary

This paper introduces a test bench for cockpit door test, and simulates the upper and lower deformation of the cockpit door, which are the two most deformed working conditions for the test bench, through the finite element software ABAQUS, and finally obtains the following conclusions:

1) Structural evaluation confirmed that maximum stress values in the column-side mounting plate (27.3 MPa), hinge-side mounting plate (40.0 MPa), and main frame (20.7 MPa) remain well below the material yield strengths (455 MPa for mounting plates, 355 MPa for main frame), with elastic deformation observed across all components and no evidence of plastic failure.;

2) Displacement analysis demonstrated that the main frame exhibits minimal deformation (maximum 0.19 mm), three orders of magnitude smaller than the 3 mm cockpit door deformation threshold. This negligible displacement profile validates the technical feasibility of integrating sensor instrumentation directly onto the main frame through customized mounting fixtures for precise door deformation monitoring.

ISSN:3007-9640 DOI: https://doi.org/10.70114/acmsr.2025.3.1.P258

References

[1] WANG Z, SUN W, SUN X. Research on cockpit door design of civil aircraft[J]. Aviation Standardization and Quality,2018(4):50-53. DOI:10.13237/j.cnki.asq.2018.04.013.

[2] An LL, Wang Y. Discussion on cockpit door design of civil aircraft based on functional hazard assessment[J]. Civil Aircraft Design and Research,2015(1):53-57. DOI:10.3969/j.issn.1674-9804.2015.01.012.

[3] Lu Z, Liu J. Improvement design of cockpit door control logic for civil aircraft based on fault tree analysis method[J]. Computer Measurement and Control,2020,28(1):44-47,53. DOI:10.16526/j.cnki.11-4762/tp.2020.01.011.

[4] Che Q, He YY, Chen WB, et al. Lightweight design of transmission bracket for a heavy truck[J]. Automobile Practical Technology,2021,46(11):41-43. DOI:10.16638/j.cnki.1671-7988.2021.011.014.

[5] K. Cao, Lin W.J, Kong Z. Optimization of simulation model based on ABAQUS for automobile front axle bench test[J]. Shandong Transportation Science and Technology,2021(6):133-136. DOI:10.3969/j.issn.1673-8942.2021.06.042.

[6] Wei CM, Yang Chang, Yan XT. Topology optimization and lightweight design of drive shafts for heavy-duty vehicles[J]. Mechanical Design and Manufacturing,2020(11):289-292,296. DOI:10.3969/j.issn.1001-3997.2020.11.071.

[7] Ma Kunlong. Short term distributed load forecasting method based on big data. Changsha: Hunan University, 2014.

[8] SHI Biao, LI Yu Xia, YU Xhua, YAN Wang. Short-term load forecasting based on modified particle swarm optimizer and fuzzy neural network model. Systems Engineering-Theory and Practice, 2010, 30(1): 158-160.